BAND GAP TUNING OF LANTHANUM-DOPED CUSCN VIA CHEMICAL WET PROCESS IN ENHANCING HTL FOR PSC

FARAH LIYANA BINTI MOHD RAHIM

MASTER OF SCIENCE IN ELECTRONICS ENGINEERING

2025

Faculty of Electronics and Computer Technology and Engineering

BAND GAP TUNING OF LANTHANUM-DOPED CUSCN VIA CHEMICAL WET PROCESS IN ENHANCING HTL FOR PSC

FARAH LIYANA BINTI MOHD RAHIM

MASTER OF SCIENCE IN ELECTRONICS ENGINEERING

2025

BAND GAP TUNING OF LANTHANUM-DOPED CUSCN VIA CHEMICAL WET PROCESS IN ENHANCING HTL FOR PSC

FARAH LIYANA BINTI MOHD RAHIM

A thesis submitted
In fulfillment of the requirements for the degree of
MASTER OF SCIENCE IN ELECTRONICS ENGINEERING

Faculty of Electronics and Computer Technology and Engineering

UNIVERSITI TEKNIKAL MALAYSIA MELAKA

2025

DECLARATION

I declare that this thesis entitled “Band Gap Tuning of lanthanum-doped CUSCN via Chemical Wet Process in Enhancing HTL for PSC” is the result of my own research except as cited in the references. The thesis has not been accepted for any degree and is not concurrently submitted in candidature for any other degree.

Signature	:	
Supervisor Name	:	Farah Liyana binti Mohd Rahim
Date	:	24/07/2025

APPROVAL

I hereby declare that I have read this thesis and in my opinion, this thesis is sufficient in terms of scope and quality for the award of Master of Science in Electronics Engineering

Signature	:	
Supervisor Name	:	Ts. Dr. Faiz bin Arith
Date	:	30/07/2025

DEDICATION

To my late father and my loving mother, even though my father is no longer here, his love and lessons continue to guide me every day. To my mother, thank you for your endless support, care, and encouragement. Your strength inspires me to keep going no matter what.

To my siblings, thank you for always being by my side. Your support, encouragement, and love have helped me through many difficult times. We have shared both happy and hard moments, and I am grateful to have you as my family.

To my teammates, I am thankful for working together and trusting each other. We have faced challenges as a team, and your friendship and cooperation have made this journey easier and more meaningful. Together, we have learned and grown.

And to myself, I want to say thank you for being strong and brave. This journey has not been easy, but I kept going because I believed in myself and the people who care about me. I am proud of how far I have come, and I will keep moving forward with hope and determination.

ABSTRACT

Perovskite Solar Cells (PSCs) have become one of the most intriguing topics in the avant-garde renewable energy due to their remarkable Power Conversion Efficiency (PCE). Hole Transport Layer (HTL) remains indispensable in all PSCs architectures as it extracts holes from the perovskite layer and subsequently transports to the electrodes while enriching contacts with other layers of the cell. Copper(I) thiocyanate (CuSCN) has garnered attention as an effective HTL in PSCs due to its advantageous electronic properties, high stability, and excellent hole mobility. Unlike the widely used Spiro-OMeTAD, which is sensitive to moisture and degrades rapidly, CuSCN offers a more stable alternative with excellent moisture resistance. CuSCN is particularly promising as it provides a robust interface with better resistance against environmental factors such as moisture, thereby enhancing the overall durability of solar cells without sacrificing efficiency. However, CuSCN's application is limited by its low hole concentration and conductivity. The CuSCN HTL still suffers from the chemical reaction at the interface, predominantly due to copper vacancies. This research introduces Lanthanum (La), a rare earth material, as a dopant that incorporates into CuSCN and acts as HTL in PSCs. The solution-processable deposition of CuSCN using dimethyl sulfoxide (DMSO) facilitates the formation of a highly transparent and stable HTL, crucial for efficient hole extraction and device durability. Experimental optimization identified an optimal La doping concentration of 3 mol%, which yielded a conductivity of 4.13 S/cm, a band gap energy of 3.67 eV, a crystallite size of 8.47 nm, a grain size of 572.50 nm, and a transmittance exceeding 40% at 500 nm of wavelength, indicating sufficient optical transparency for effective light harvesting. These parameters indicate improved charge transport and film quality, which are essential for high-performance PSCs. Using the SCAPS-1D simulation tool, the study further modeled the La-doped CuSCN-based PSC incorporating the experimentally derived parameters. $MAPbI_3$ (methylammonium lead iodide) was used as the absorber layer, TiO_2 (titanium dioxide) as ETL, Indium Tin Oxide (ITO), and gold as front and back contact. From the simulation, the fully optimized device structure, ITO/TiO_2/$MAPbI_3$/La-dopedCuSCN/Au attained remarkable PCE of 30.39%, with a fill factor (FF) of 83.63%, short-circuit current density (Jsc) of 25.163 mA/cm^2, and open-circuit voltage (Voc) of 1.2629 V. Additionally, the simulation explored the influence of various factors such as HTL thickness, doping density, interface defect density, and operating temperature on device performance, allowing for comprehensive optimization. Overall, this work demonstrates that La doping in CuSCN significantly enhances the electrical and interfacial properties of the HTL, leading to improved PSC efficiency and stability.

PENALAAN SELAR JALUR CUSCN BERDOP LANTANUM MELALUI PROSES BASAH KIMIA DALAM PENAMBAHBAIKAN HTL UNTUK PSC

ABSTRAK

Sel Suria Perovskite (PSC) telah menjadi salah satu topik yang paling menarik dalam bidang tenaga boleh diperbaharui kerana Kecekapan Penukaran Kuasa (PCE) yang luar biasa. Lapisan Pengangkut Lubang (HTL) kekal sebagai komponen penting dalam semua seni bina PSC kerana ia mengekstrak lubang (holes) daripada lapisan perovskite dan seterusnya mengangkutnya ke elektrod, di samping memperkukuh hubungan dengan lapisan-lapisan lain dalam sel. Kuprum(I) tiosianat (CuSCN) telah mendapat perhatian sebagai HTL yang berkesan dalam PSC kerana sifat elektroniknya yang bermanfaat, kestabilan yang tinggi dan mobiliti lubang yang cemerlang. Berbeza dengan Spiro-OMeTAD yang digunakan secara meluas tetapi sensitif terhadap kelembapan dan mudah terdegradasi, CuSCN menawarkan alternatif yang lebih stabil dengan ketahanan kelembapan yang baik. CuSCN amat berpotensi kerana ia menyediakan antara muka yang kukuh dengan ketahanan yang lebih baik terhadap faktor persekitaran seperti kelembapan, sekali gus meningkatkan ketahanan keseluruhan sel suria tanpa mengorbankan kecekapan.Walau bagaimanapun, aplikasi CuSCN terhad oleh kepekatan lubang dan kekonduksian yang rendah. HTL CuSCN masih terjejas oleh tindak balas kimia pada antara muka, terutamanya disebabkan oleh kekosongan kuprum. Kajian ini memperkenalkan Lanthanum (La), sejenis bahan nadir bumi, sebagai dopan yang dimasukkan ke dalam CuSCN dan bertindak sebagai HTL dalam PSC. Pemendapan CuSCN yang boleh diproses melalui larutan menggunakan dimetil sulfoksida (DMSO) memudahkan pembentukan HTL yang sangat telus dan stabil, yang penting untuk pengekstrakan lubang yang cekap dan ketahanan peranti.Pengoptimuman eksperimen mengenal pasti kepekatan doping La optimum sebanyak 3 mol%, yang menghasilkan kekonduksian 4.13 S/cm, selar jalur (band gap) 3.67 eV, saiz kristalit 8.47 nm, saiz butiran 572.50 nm, dan transmisi yang melebihi 40% pada panjang gelombang 500 nm, menunjukkan ketelusan optik yang mencukupi untuk penuaian cahaya yang berkesan. Parameter-parameter ini menunjukkan peningkatan dalam pengangkutan cas dan kualiti filem, yang penting untuk PSC berprestasi tinggi. Menggunakan alat simulasi SCAPS-1D, kajian ini turut memodelkan PSC berasaskan CuSCN yang didop La dengan menggabungkan parameter yang diperoleh secara eksperimen. $MAPbI_3$ (metilammonium plumbum iodida) digunakan sebagai lapisan penyerap, TiO_2 (titanium dioksida) sebagai ETL, manakala Indium Tin Oxide (ITO) dan emas digunakan sebagai sentuhan hadapan dan belakang. Hasil simulasi menunjukkan struktur peranti yang dioptimumkan sepenuhnya, $ITO/TiO_2/MAPbI_3$/La-dopedCuSCN/Au, mencapai PCE yang luar biasa sebanyak 30.39%, dengan faktor isian (FF) 83.63%, ketumpatan arus litar pintas (Jsc) 25.163 mA/cm², dan voltan litar terbuka (Voc) 1.2629 V. Selain itu, simulasi turut mengkaji pengaruh pelbagai faktor seperti ketebalan HTL, ketumpatan doping, ketumpatan kecacatan antara muka, dan suhu operasi terhadap prestasi peranti, membolehkan pengoptimuman secara menyeluruh. Secara keseluruhannya, kajian ini menunjukkan bahawa doping La dalam CuSCN meningkatkan dengan ketara sifat elektrik dan antara muka HTL, yang membawa kepada peningkatan kecekapan dan kestabilan PSC.

ACKNOWLEDGEMENT

In the name of Allah, the Most Gracious, the Most Merciful.

First and foremost, I would like to express my profound gratitude to my supervisor, Ts. Dr. Faiz Arith, for his exceptional guidance, unwavering support, and invaluable insights throughout this research. His expertise and constructive feedback have been fundamental in shaping the direction and quality of this work.

I am also sincerely thankful to my research team members for their dedicated assistance and collaborative spirit. Their professionalism and expertise have significantly contributed to the successful completion of this study.

I would like to express my deepest gratitude to the technical staff for their continuous support and assistance. Their expertise in operating the equipment, solving technical problems, and who assist me perform the characterization has facilitated the progress of this research. I wish to extend my deepest appreciation to my family for their steadfast encouragement, patience, and understanding. Their continuous support has been a source of motivation and strength during the most demanding phases of this endeavor.

Finally, I acknowledge with gratitude all individuals and institutions whose support, whether direct or indirect, has facilitated this research. Your contributions have been instrumental in bringing this project to fruition. May Allah bless you all abundantly.

TABLE OF CONTENTS

ABSTRACT **i**
ABSTRAK **ii**
ACKNOWLEDGEMENT **iii**
TABLE OF CONTENTS **iv**
LIST OF TABLES **vi**
LIST OF FIGURES **vii**
LIST OF ABBREVIATIONS **x**
LIST OF SYMBOLS **xiii**
LIST OF APPENDICES **xv**
LIST OF PUBLICATIONS **xvi**

CHAPTER

1. INTRODUCTION **1**
- 1.1 Background 1
- 1.2 Problem Statement 4
- 1.3 Research Objective 6
- 1.4 Scope of Research 6
- 1.5 Research Hypothesis 7
- 1.6 Thesis Outline 8
- 1.7 Summary 9

2. LITERATURE REVIEW **11**
- 2.1 Introduction 11
- 2.2 Renewable Energy 12
- 2.3 Generation of solar cells 13
  - 2.3.1 First Generation Solar Cell 15
  - 2.3.2 Second Generation Solar Cell 16
  - 2.3.3 Third Generation Solar Cell 17
- 2.4 Solar Terminology 21
  - 2.4.1 Series Resistance (Rs) 22
  - 2.4.2 Shunt Resistance (R_{SH}) 23
  - 2.4.3 Open-Circuit Voltage (V_{OC}) 23
  - 2.4.4 Short-Circuit Current (I_{SC}) 24
  - 2.4.5 Fill Factor (FF) 24
  - 2.4.6 Power Conversion Efficiency (ŋ) 25
- 2.5 Perovskites Solar Cells 26
  - 2.5.1 Working Principle of PSC 29
  - 2.5.2 Electron Transport Layer (ETL) 32
  - 2.5.3 Hole Transport Layer (HTL) 34
- 2.6 CuSCN as HTM 36
  - 2.6.1 CuSCN as HTL 39
  - 2.6.2 Fabrication Techniques in CuSCN 41
- 2.7 Doping 45

2.7.1 General Doping Approaches in HTLs 45
2.7.2 Rare Earth dopants in PSCs 46
2.8 Summary 52
3. METHODOLOGY **53**
3.1 Introduction 53
3.2 Experimental Method 55
3.2.1 Cleaning Substrate 55
3.2.2 Synthesis of La-doped CuSCN Film 57
3.2.3 Characterization of La-doped CuSCN Films 60
3.2.4 Theoretical Calculation 65
3.3 PSC Device Simulation 66
3.3.1 SCAPS-1D 3.3.11 Software 66
3.3.2 Simulation Flowchart of SCAPS-1D 70
3.3.3 PSC Design Structure 72
3.4 Summary 75
4. RESULT AND DISCUSSION (Experimental) **76**
4.1 Experimental Result 76
4.1.1 Structural Properties 76
4.1.2 Chemical Properties 85
4.1.3 Optical Properties 91
4.1.4 Electrical Properties 96
4.2 Summary 99
5. RESULT AND DISCUSSION (SIMULATION) **101**
5.1 Optimization of La-doped CuSCN as HTL 102
5.1.1 Influence of HTL Thickness Variation 102
5.1.2 Influence of HTL Doping Acceptor Density Variation 104
5.1.3 Influence of Defect Density at HTL/Absorber Interface 106
5.2 Optimization of TiO_2 as ETL 107
5.2.1 Influence of ETL Thickness Variation 107
5.2.2 Influence of ETL Doping Donor Density 109
5.2.3 Influence of ETL Defect Density Absorber / ETL 111
5.3 Optimization of $MAPbI_3$ as absorber layer 112
5.3.1 Influence of Absorber Layer Thickness Variation 112
5.3.1 Influence of Absorber Layer Doping Acceptor Density 115
5.4 Optimization of temperature in PSC 116
5.5 Final Optimization of PSC 118
5.6 Summary 120
6. CONCLUSION AND RECOMMENDATIONS FOR FUTURE RESEARCH **121**
6.1 Summary 121
6.2 Recommendation for Future Research 124
REFERENCES **125**
APPENDICES **143**

LIST OF TABLES

TABLE	TITLE	PAGE
Table 2.1	Summary of CuSCN films for solar applications	44
Table 2.2	The summary of dopants in CuSCN in solar cell applications	50
Table 2.3	Photovoltaic parameters of PSCs with TiO_2 and La/TiO_2 (Gao et al., 2016)	52
Table 2.4	Summary of the La as dopants in solar cell applications.	51
Table 3.1	Amount of La for various molar concentrations	60
Table 3.2	Input parameters of the La-doped CuSCN-based	75
Table 3.3	Input parameters of the interface layer of PSC	76
Table 4.1	The value of the crystallite size and lattice constant for various La doping concentrations	85
Table 4.2	Summary of binding energy values from XPS analysis of La-doped CuSCN at various La concentrations	90
Table 4.3	The value of transmittance and band gap for various mol% of La doping concentrations	93
Table 4.4	The value of conductivity, resistivity, and sheet resistance for various La doping concentrations	98

LIST OF FIGURES

FIGURE	TITLE	PAGE
Figure 1.1	The p–n junction of photovoltaic device	2
Figure 2.1	Chart on conversion efficiencies of the research cells, published by the National Renewable Energy Laboratory (NREL) (NREL, 2025)	14
Figure 2.2	Mono-crystalline & Poly-crystalline cells (Dhilipan et al., 2022)	16
Figure 2.3	Copper Indium Gallium Diselenide (CIGS) cells	17
Figure 2.4	Dye-sensitized solar cells (DSSC) (Ranabhat et al., 2016)	20
Figure 2.5	Perovskite Solar Cells (PSCs) (Ronn Andriessen, 2019)	20
Figure 2.6	The current voltage (IV) of solar cells	22
Figure 2.7	Perovskites typically consist of a cubic lattice form (Chung et al., 2012)	27
Figure 2.8	The PSC structure diagram	28
Figure 2.9	Carriers generation (electron-hole pair) in semiconductor	30
Figure 2.10	The band alignment diagram displays the generation of excitons and carries transport states formed by photon absorption	32
Figure 2.11	(a) α-phase (orthorhombic); (b) β-phase (hexagonal) (Pattanasattayavong et al., 2017)	37
Figure 2.12	The spin coating method (Aliyaselvam et al., 2025)	42
Figure 2.13	The doctor blade method (Frederichi et al., 2020)	43
Figure 2.14	Top-view SEM micrographs of the (a) pristine and (b) F_4TCNQ-doped films	48
Figure 3.1	Research flowchart	54
Figure 3.2	Indium-doped tin oxide (ITO) glass substrates	56
Figure 3.3	Cleaning process in an ultrasonic bath	56
Figure 3.4	The fabrication process of La-doped CuSCN film	58

Figure 3.5	The solution on the magnetic stirrer	58
Figure 3.6	La-doped CuSCN solution was dripped onto ITO glass	69
Figure 3.7	The sample was annealed in the oven at 100 °C	69
Figure 3.8	Equipment used in characterization (a) field-emission scanning electron microscope (FESEM, SU5000 from Hitachi); (b) X-ray diffraction (XRD); (c) Ultraviolet-visible spectroscopy (UV-vis, Shimadzu UV-1700); (d) I-V characteristics (Keithley 2401 source meter) (e) X-ray Photoelectron Spectrometer (K-Alpha)	64
Figure 3.9	Action Panel	67
Figure 3.10	Solar Cell Definition Panel	68
Figure 3.11	SCAPS-1D 3.3.11 Software	68
Figure 3.12	Simulation flowchart of SCAPS 1D Software	71
Figure 3.13	The structure of PSC	73
Figure 3.14	The band alignment of the simulated PSC device structure	73
Figure 4.1	The cross-sectional of the FESEM image.	77
Figure 4.2	Top view FESEM images reef-like structure of La-doped CuSCN at different molar concentrations at ~3500 × magnifications, a) 0 mol%, b) 1 mol%, c) 2 mol%, d) 3 mol%, e) 4 mol%, and f) 5 mol%.	79
Figure 4.3	The grain size distribution for La-doped CuSCN at various molar concentrations of La	81
Figure 4.4	XRD pattern for variation molar concentration of La-doped CuSCN	84
Figure 4.5	XPS spectra of the a) Cu 2p b) S 2p c) C 1s d) N 1s regions of La-doped CuSCN films by varying mol% concentrations	86
Figure 4.6	XPS spectra of the La regions of La-doped CuSCN films by varying mol% concentrations	89
Figure 4.7	Absorbance spectra of CuSCN thin films with different molar concentrations of La.	92

Figure 4.8	Trasmittance spectra of CuSCN thin films with different molar concentrations of La.	93
Figure 4.9	The tauc plot of La-doped CuSCN at different molar concentrations of La (inset: the band gap at various molar concentrations of La)	95
Figure 4.10	The electrical properties of La-doped CuSCN with various molar concentrations	98
Figure 5.1	The variation of La-doped CuSCN thickness of simulated PSC	103
Figure 5.2	The variation of La-doped CuSCN doping acceptor density of simulated PSC	104
Figure 5.3	The variation of La-doped interface defect density CuSCN/$MAPbI_3$ of simulated PSC	107
Figure 5.4	The variation of TiO_2 thickness of simulated PSC	108
Figure 5.5	The variation of TiO_2 ETL doping donor density of simulated PSC	110
Figure 5.6	The variation of interface defect density $MAPbI_3$ / TiO_2 of simulated PSC	112
Figure 5.7	The variation of $MAPbI_3$ thickness of simulated PSC.	114
Figure 5.8	The variation of $MAPbI_3$ doping acceptor density of simulated PSC	116
Figure 5.9	The variation of temperature of simulated PSC	117
Figure 5.10	J-V curve before and after optimization using SCAP-1D software for La-doped CUSCN PSCs.	119

LIST OF ABBREVIATIONS

PV	-	Photovoltaic
PSC	-	Perovskite solar cells
CuSCN	-	Copper Thiocyanate
La	-	Lanthanum
HTL	-	Hole Transport Layer
ITO	-	Indium Tin Oxide
XRD	-	X-ray Diffraction
FESEM	-	Field Emission Scanning Electron Microscopy
PCE	-	Power conversion efficiency
ETL	-	Electron Transport Layer
R_s	-	Series Resistance
FF	-	Fill Factor
J_{sc}	-	Short-circuit density
Voc	-	Open-circuit voltage
R_{sh}	-	Shunt Resistance
Isc	-	Short-circuit current
P_{max}	-	Maximum power output
P_{IN}	-	Product of power input
Gss	-	Grid Sub-Station
DER	-	Distributed Energy Resorces
$CaTiO_3$	-	Calcium titanate
CH_3NH_3	-	Methylammonium
$CH(NH_2)^{2+}$	-	Formamidinium

Cl^-	-	Chlorine Ion
Br^-	-	Bromine Ion
TiO_2	-	Titanium dioxide
Pb^{2+}	-	Lead Ion
Sn	-	Tin
Al_2O_3	-	Aluminium oxide
DSSCs	-	Dye-sensitized solar cells
FTO	-	Fluorine-doped tin oxide
Au	-	Gold
Ge	-	Germanium
ZnO	-	Zin oxide
PCBM	-	[6,6]-phenyl-C 61 -butyric acid methyl ester
PFN	-	9,9-dioctylfluorene-9,9-bis (N, N-imethylpropyl)fluorene
HOMO	-	Highest occupied molecular orbit
LiTFSI	-	bis(trifluoromethane) sulfonimide lithium
PTAA	-	poly[bis(4-phenyl)(2,4,6-trimethylphenyl)amine]
$MAPbI_3$	-	Methylammonium lead iodide
P3HT	-	Poly(3-hexylthiophene)
PEDOT: PSS	-	Poly(3,4-ethylenedioxythiophene) polystyrene sulfonate
PCDTBT	-	Poly[N-9′-heptadecanyl-2,7-carbazole-alt-5,5-(4′,7′-di-2-thienyl-2′,1′,3′-benzothiadiazole)]
PCPDTBT	-	Poly[2,6-(4,4-bis-(2-ethylhexyl)-4H-cyclopenta[2,1-b;3,4-b]dithiophene)-alt-4,7(2,1,3-benzothiadiazole)]
CuI	-	Copper Iodide
NiO	-	Nickel (II) oxide
$CsSnI_3$	-	Cesium triiodostannate (II)

HTM	-	Hole transport material
SnO	-	Tin (II) oxide
DES	-	Diethyl sulfate
DMS		Dimethyl sulfate
$CH_3NH_3PbI_3$	-	Methylammonium lead halide
rGO	-	Reduced Graphine oxide
SSDSC	-	Solid-state dye-sensitived solar cell
O_2	-	Dioxygen
Cu	-	Copper
TrTPFB	-	trityl tetrakis(pentafluorophenyl)borate
OLEDs	-	organic light-emitting diode
F_4TCNQ	-	2,3,5,6-Tetrafluoro-7,7,8,8-tetracyanoquinodimethane
PVK	-	poly-N-vinylcarbazole
Li	-	Lithium
$C_{60}F_{48}$	-	Fluorinated Fullerene
$SrSnO_3$	-	Strintium tin oxide
CO	-	Carbon monoxide
DI	-	Deionized
DMSO	-	Dimethyl sulfoxide
MEA	-	Monoethanolamine
FWHM	-	Full Width Half Maximum

LIST OF SYMBOLS

τ_n	-	Lifetime of Electron
τ_p	-	Lifetime of Hole
D	-	Diffusion Coefficient
q	-	Electron of Charge
$n(x)$	-	Concentration of Free Electrons
Ψ	-	Electrostatic Potential
$N_A^-(x)$	-	Concentration Of Ionized Acceptor
$p(x)$	-	Concentration of Free Holes
$n_t(x)$	-	Concentration Trapped Electron
x	-	Direction along The Thickness
$N_v^+(x)$	-	Concentration of Ionized Donor
$p_t(x)$	-	Concentration Trapped Hole
d	-	Layer Thickness
E_g	-	Band Gap Energy
ε	-	Dielectric Permittivity
N_{VB}	-	Effective Density of State Valence Band
N_{CB}	-	Effective Density of State Conduction Band
V_e	-	Thermal Velocity of Electrons
V_h	-	Thermal Velocity of holes
μ_e	-	Electron Mobility
μ_h	-	Hole Mobility

N_D	-	Density Of Donors
N_A	-	Density Of Acceptors
$°C$	-	Temperature
mol%	-	Mole percent concentration of a component in a mixture
$E_g\,(eV)$	-	Band gap energy
$X\,(eV)$	-	Electron affinity
β	-	Full width at half maximum
μm	-	Micrometer
λ	-	X-ray wavelength
A	-	Absorbance
T	-	Transmittance
2θ	-	Bragg diffraction angle
φ	-	Metal work function
φ_b	-	Schottky barrier height
g/mol	-	Molecular mass
$\varepsilon/\varepsilon_o$	-	Dielectric permittivity

LIST OF APPENDICES

APPENDIX	TITLE	PAGE
Appendix A	Material experimental	131
Appendix B	XRD default file for CuSCN	132
Appendix C	Cross-sectional FESEM La-doped CuSCN	134

LIST OF PUBLICATIONS

The following are the list of publications related to the work on this thesis:

Main Author

F. Rahim, F. Arith, N. Izzati, N. A. Jalaludin, F. Salehuddin. A.S.M. Shah A.N. Mustafa, "Computational study of highly efficient SnO_2 ETL-based inorganic perovskite solar cell" *Przeglad Elektrotechniczny*. vol. 11, pp. 101–105, 2024. (Scopus and ESCI WoS Indexed)

Co-author

N. A. Jalaludin, **F. Rahim**, F. Arith, F. Salehuddin. A.N. Mustafa, K.E. Kharudin, M.A. Islam, and N. Amin "Efficient Hole Extraction by Doped-Polyaniline/Graphene Oxide in Lead-Free Perovskite Solar Cell: A Computational Study. *Physica Scripta*. 100 (2), 2025. (Scopus and Q2 WoS Indexed, IF=2.6

CHAPTER 1

INTRODUCTION

This chapter presents an overview of the research, detailing the research objectives and problem statement. It also defines the scope of the project, outlining the limitations and specifying the features and functions of the expected research outcomes. Additionally, the research hypothesis, a fundamental component of the scientific method, is introduced to propose the anticipated results of the experiments.

1.1 Background

Solar cells, which are also commonly referred to as photovoltaic (PV) cells, are specialized devices designed to convert sunlight directly into electrical energy through the photovoltaic effect (Baghzouz, 2015). This innovative technology plays a vital role in the global transition toward renewable energy sources by providing a clean, sustainable, and environmentally friendly alternative to traditional fossil fuels, which are finite and contribute to pollution and climate change. Although the fundamental concept of photovoltaic cells was first discovered in the 19th century, it was not until the 20th century that significant technological advancements and practical applications began to emerge (Pastuszak et al., 2022) . Over the decades, solar cell technology has undergone continuous improvement, evolving from early models characterized by relatively low energy conversion efficiencies to modern, highly efficient designs that are both more effective at capturing solar energy and increasingly cost-competitive with conventional energy sources.

The underlying structure of most solar cells is primarily based on semiconductor materials, with silicon being the most widely used due to its natural abundance, well-established manufacturing processes, and excellent ability to absorb sunlight and convert it into electricity. Typically, a solar cell consists of two distinct layers of silicon, one doped to create a p-type semiconductor and the other doped to form an n-type semiconductor. These two layers come together to form a p-n junction, which is essential for creating an internal electric field that drives the movement of charge carriers when the cell is exposed to sunlight. In addition to these basic layers, modern solar cells often incorporate several other functional layers, such as antireflection coatings that minimize the loss of incoming light due to reflection, as well as electrical contact layers that facilitate the efficient collection and transport of generated electrical current (Baghzouz, 2015). The p-n junction in Figure 1.1 serves as the core region where the photovoltaic effect takes place: when photons from sunlight strike the solar cell, they excite electrons within the semiconductor material, generating electron-hole pairs. The internal electric field at the junction then separates these charge carriers, causing electrons to flow through an external circuit and thereby producing usable electrical power.

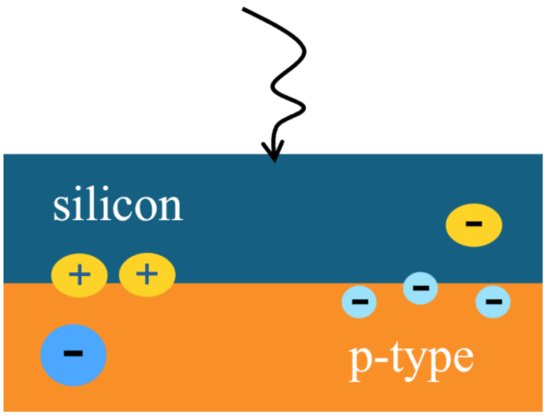

Figure 1.1: The p–n junction of photovoltaic device